EFFECTS ON URBAN FOUNDATIONS OF SOIL-MOISTURE CHANGES CAUSED BY TREES

V. Navarro, M. Candel, A. Yustres, B. García

Departamento de Ingeniería Civil y de la Edificación, U. de Castilla-La Mancha, Edificio Politécnico Avda. Camilo José Cela s/n, 13071, Ciudad Real, vicente.navarro@uclm.es.

ABSTRACT. Trees growing close to buildings in urban landscapes may change soil moisture around foundations, producing shrinkage and swelling. We present a numerical solver which enables us to evaluate the movements resulting from these volumetric strains. This tool will be of assistance both in designing the foundations of new buildings, and in the analysis of damage associated with buildings that have already been constructed.
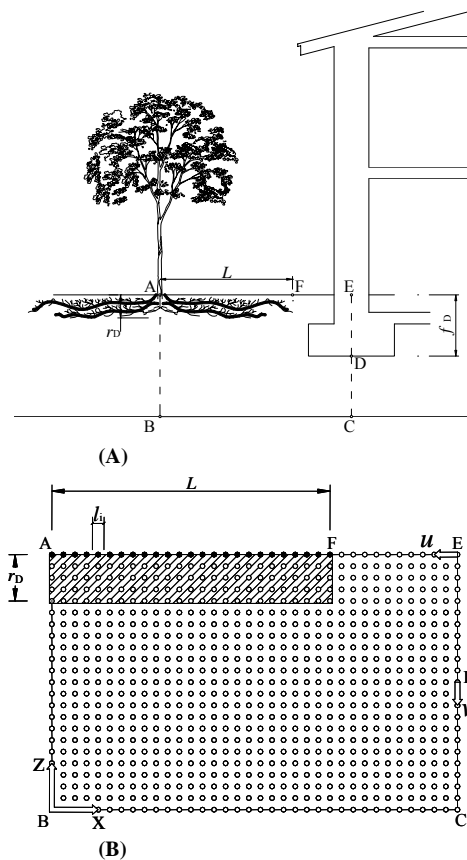
RESUMEN. Los árboles plantados cerca de edificios en ambientes urbanos producen cambios en la humedad del suelo en el entorno de las cimentaciones, dando lugar a procesos de hinchamiento y retracción. Este artículo presenta un módulo numérico que permite la evaluación de los movimientos causados por la deformación volumétrica del suelo. Esta herramienta servirá de ayuda para el proyecto de las cimentaciones y para el análisis del daño en edificios ya existentes,

1.- Introduction

The amount of water supplied by rainfall in urban landscapes is often lower than the quantity transpired by trees, especially in the dry-growing seasons (Canada Mortgage and Housing Corporation (CHMC), 2005). Under these conditions, soil moisture around trees gradually diminishes, producing an increase in matric suction that causes the soil to shrink. When tree activity ceases, the opposite phenomenon may occur and the soils may swell. In some soils, the volumetric strains associated with these processes may be important, affecting a considerable area around the tree. The longer the drought, the higher the strains, and the farther the tree influence zone will extend. Therefore, the higher the risk that trees will damage nearby buildings.

A well-established set of rules of thumb is used to prevent this kind of damage at present (National House Building Council (NHBC), 1997; Zurich Municipal, 1996; British Standard (BS), 1991; Building Research Establishment (BRE), 1996; Building Research Establishment (BRE), 1999). However, it is not common to attempt to reproduce shrink-swell processes. Both

processes depend not only on the proximity of trees to houses, but also on the arrangement of the materials that make up the foundation ground, the stiffness of these materials when subjected to suction changes, soil hydraulic behaviour and the way in which trees take up water from the ground. Unsaturated Soil Mechanics currently offers theoretical and computational tools that are able to successfully tackle the problem (Alonso and Lloret, 1995). These tools, however, usually require a high level of detail in terms of domain characterization which calls for an experimental effort that is generally beyond the scope of building technology, especially when low rise buildings are involved. For this reason, it is of interest to find approximate solutions that

Fig. 1. A) Analyzed cross-section. B) Space discretization. The shaded area identifies the zone where vertical permeability is assumed to be greater than horizontal permeability. Boundary conditions are defined in table 1.

will make it possible to outline the processes, carry out sensitivity analyses and provide a general quatitative idea, of the effect trees have on building foundations. This paper aims at offering a solution of this type.

2.- Idealization of the problem and conceptual basis

Of the many different possible configurations, the simple plane flow problem depicted in Fig. 1 with the boundary conditions shown in Table 1 was chosen for the type case study. Water uptake Q by the tree was simulated by means of "sink-points", which model the large-sized or main roots. The geometry portrayed in Fig. 1 (where L indicates the main root length, while r_D defines the root depth, and f_D is the foundation depth) was used to take into account that urban trees often take advantage of the fill generally found between the subgrade soil and the pavement as the preferred channel for growth.

**Table 1.** Model boundary conditions (see figure 1 B).

	Boundary Conditions
AB	No flow
BC	Water table
CE	Impervious
EF	Impervious
FA	"Sink-points" (main roots)

The roots did not develop their radicular mass in the fill, which has a low water content, and presented serious impediments to the flow in partially saturated conditions. However, the fill-subgrade soil interface served as a medium for the expansion of the main roots from which the tree sent out a second hierarchy of roots towards the soil to absorb water. This "urban root distribution" is different from the one adopted by Indraratna et al. (2006) in their comprehensive study of tree root effects, and the root water uptake is estimated in a distinct and simpler way. Q was calculated by means of:

$$Q = K_{cb}(t) \cdot ET_o(t) \cdot \sum_{i=1}^{N(t)} (TLF_i \cdot A_i) \qquad (1)$$

where K_{cb} is the basal crop coefficient, ET_o is the reference evapotranspiration, TLF_i is the tree limiting factor (a water stress coefficient that indicates the decreasing evapotranspiration of the tree as the suction of the soil water increases) associated with the i-th sink-point, and A_i is the area of influence of this point (see Fig. 2). The dependence of the number of sink-points N upon time t would indicate that the number of sink-points increases with the growth of the main root. This growth may be estimated on the basis of the canopy growth. So, for broad trees, a main root length / canopy diameter ratio of 1.5 (Odenwald and Welch, 2004) may be used as a preliminary estimation. In the numerical solver, which we will call 2NSAT, more complicated growth models can be introduced relatively easily (Mathur, 1999). In keeping

with the work done by Tratch et al. (1995), the TLF was simulated by means of the logarithmic law proposed by Feddes et al. (1978) .TLF= 1 was used for suctions of less than 100 kPa, and TLF=0, for suctions reaching 1500 kPa (the conventional wilting point value). The value of product $K_{cb} \cdot ET_o$ must be entered by the user. 2NSAT will accept variations in $K_{cb} \cdot ET_o$ over the course of time. Thus Fig. 3, for example, presents the variation in $K_{cb} \cdot ET_o$ used in the application example discussed in section 3 (the 6-month mean value was defined on the basis of meteorological data supplied by a weather station located near the study area). It is a typical case where evapotranspiration is expressed schematically assuming that there is a dormant period of 6 months ($K_{cb} \cdot ET_o$=0), followed by 6 months of activity during which a mean value of $K_{cb} \cdot ET_o$ is used. In more detailed studies, the variation in evapotranspiration can be defined with greater precision. Moreover, by default, during the active season, a nocturnal stoppage of 8 hours is introduced.
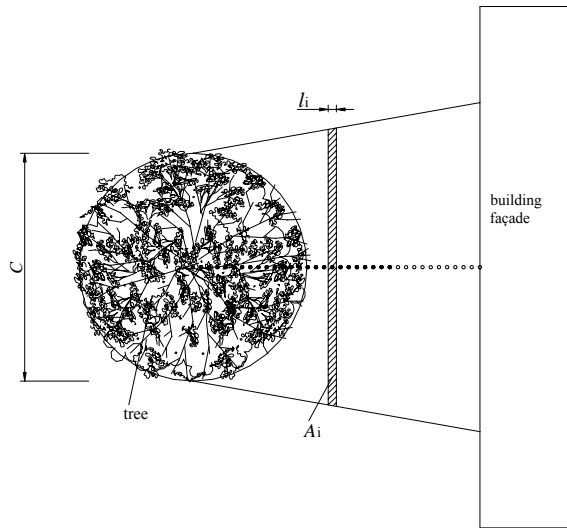
Fig 2. Area of influence Ai of each sink-point. Plane view. The sink-points are depicted in black. li is defined in figure 1 b. C is the canopy diameter.
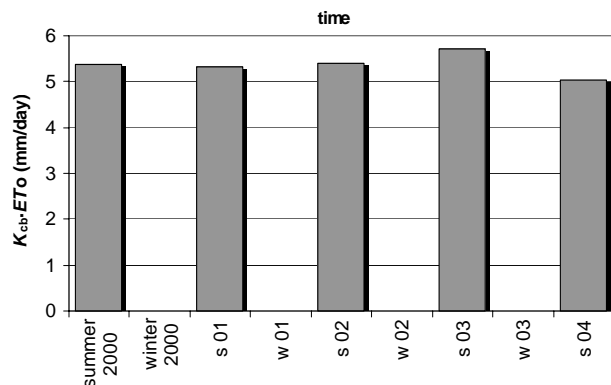
Fig. 3. Variation of the tree evapotranspiration considered in the analysis carried out in Rondilla Street (Alcázar de San Juan, central Spain).

In 2NSAT, the water flow is described by a generalized

Darcy's equation:

$$\boldsymbol{q} = -\frac{K \cdot \kappa}{\mu}\left(\nabla P + \gamma \nabla z\right) \tag{2}$$

where $\boldsymbol{q}$ is the seepage vector, P is the water pressure, z is the vertical coordinate, K, is the intrinsic permeability $[L^2]$, κ is the relative permeability, and μ and γ are, respectively, dynamic viscosity and the specific weight of water. The relative permeability is computed combining the Brooks and Corey (1964) and Burdine (1953) models:

$$\kappa = Se^{3+2/\lambda} \tag{3}$$

where the effective saturation Se is defined as:

$$Se = \frac{(\theta - \theta_R)}{(\theta_S - \theta_R)} \tag{4}$$

θ being the volumetric water content, and θ_R and θ_S, the residual and the saturated water content, respectively. The effective saturation is calculated by means of van Genuchten's (van Genuchten, 1980) water retention relationship:

$$Se = \left(1 + (\alpha \cdot s)^n\right)^{-m} \tag{5}$$

where s is the matric suction ($s=P_G-P$, P_G being the gas pressure), α is a fitting parameter related to air entry pressure, and both n and m are fitting parameters related to pore size distribution. The relationship $m=1-1/n$ is assumed. Also assumed is the Carsel and Parrish (1988) equivalence between the fitting parameter λ of Eq. (3) and the van Genuchten parameter n, i.e. $\lambda=n-1$. Parameters K, θ_S, θ_R, α and m may be estimated using the mean values proposed by Meyer et al. (1999). However, the quality of the model increases if the parameters are obtained experimentally. Thus, in the case given in section 3, the parameters were identified based on the results from six swelling tests (see Table 2).

Isothermal flow is considered. Moreover, we assume that air voids are interconnected in the field. Therefore, each build-up in gas pressure rapidly vanishes, so that gas pressure P_G remains at a constant atmospheric pressure, P_{ATM}. Consequently, only the water flow must be solved, with P being the state variable of the problem. To solve P, in 2NSAT the mass balance is formulated as follows (Navarro y Alonso, 2000):

$$\frac{\partial}{\partial t}\left((1+e)\,\theta\right) = -(1+e)\left(\nabla \cdot \mathbf{q} + r\right) \tag{6}$$

where e is the void ratio (volume of voids/volume of solid), "$\nabla \bullet$" defines the divergence operator, and r is a sink term related to the water uptake Q. In these computations, e is not constant. A logarithmic state

surface model is considered (see, for example, Lloret and Alonso, 1985) to define the volumetric strain, ε_V:

$$\varepsilon_V = C_h \cdot log(s + P_{ATM}) \tag{7}$$

where C_h is the suction compression index, also obtained in the case presented in section 3 from the results of the swelling tests (see Table 2). If experimental data are not available, the swell potential defined by Seed et al. (1962) (see Fig. 4) may be identified with the expansiveness classification of Mc Keen (1992), subsequently using the values put forth by Mc Keen (1992) to estimate C_h (see Table 3).

Table 2. Definition of the problem solved to obtain figure 5. The parameters were identified on the basis of the results from the swelling tests.

Geometry (see figure 1)	
AF (m)	0.45
FE (m)	2.55
ED (m)	0.4
DC (m)	2.8
Material Parameters	
K (m^2)	1.54×10^{-14}
θ_R	0.08
θ_S	0.43
α	0.104
n	1.23
C_h	0.006
Boundary Conditions (see figure 1)	
AB	Impervious
BC	suction $s=0$ (water table)
CE	impervious
EF	impervious
FA	suction $s=200$ kPa

Specifically, 2NSAT calculates by default the horizontal deflection u at contact point E of the ground level with the building façade (see Fig. 1), and the vertical movement v at point D. It must be identified by the user by its coordinate z, and it is generally recommended to be taken at the base of the building footing (Fig. 1). The values of u and v are written (see Fig. 5) for observation times that must be defined by the program user. In Fig. 6, are also given in these times the distribution of the matric suction and the water content in the domain. To obtain this figure, the material parameters and geometry from Table 2 were used. The boundary conditions are defined in Table 1, using the evapotranspiration defined in Fig. 3 for the sink-points.
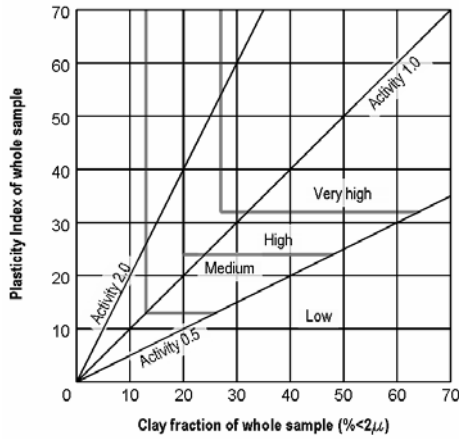
Fig. 4. Swell potential as a function of clay fraction and Plastic Index (adapted from Seed et al., 1962).
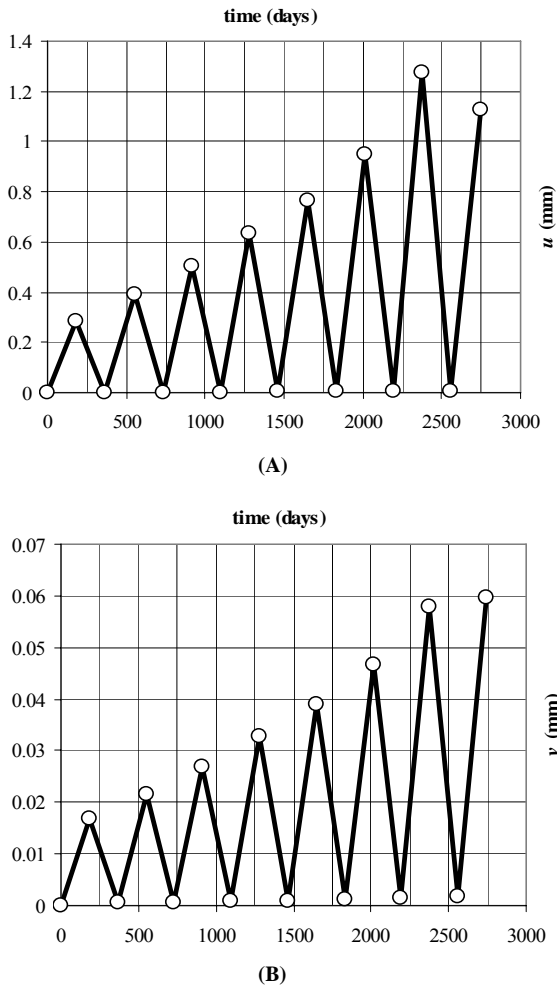

(A)

(B)

Fig. 5. A) Horizontal deflections u (see figure 1) obtained from the simulation associated with Fig. 6. B) Vertical movements v (figure 1) obtained in the same simulation.
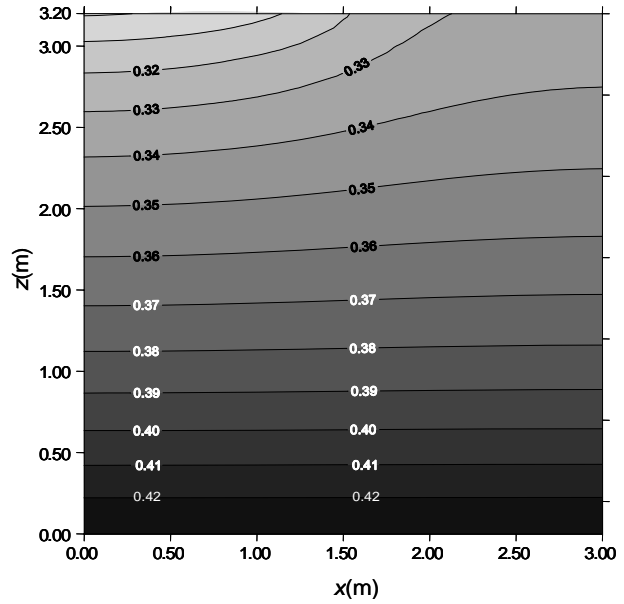

Fig. 6. Estimation of the water content distribution around a chinaberry tree located close to building #136 in Rondilla Street. The results pertain to the summer of 2004.

3.- Verification and application of the model

While the simple structure of 2NSAT makes verification easy, it becomes even more straight-forward if the program is modified by taking a linear retention curve, and assuming a constant relative permeability. Hence, even if a suction or a constant flow are imposed along AE (see Fig. 1), the boundary problem is almost 1D, and has a closed-form solution. Thanks to these solutions, we have been able to make the preliminary verifications of 2NSAT. Solutions obtained with other codes were used to validate the code when more complex boundary conditions and flow models were considered. Hence, Fig. 7 presents a comparison of the solutions obtained using 2NSAT and SEEP/W (Geo-Slope, 2002) after solving the problem defined in Table 2. A hydrostatic suction distribution was assumed to define the initial condition. AF was assumed to have a suction of 200 kPa, while boundary FE was assumed to be impervious. An isotropic permeability is adopted. The results of the 504 grid points are compared, resulting in a highly satisfactory square of Pearson's correlation coefficient of 99.7 %.

Table 3. Suction compression index C_h and soil expansiveness classifications proposed by McKeen (1992).

expansiveness classification	C_h
Very high	0.277
High	0.120 to 0.277
Moderate	0.040 to 0.120
Low	0 to 0.040
non-expansive	0

suction (kPa) - SEEP/W
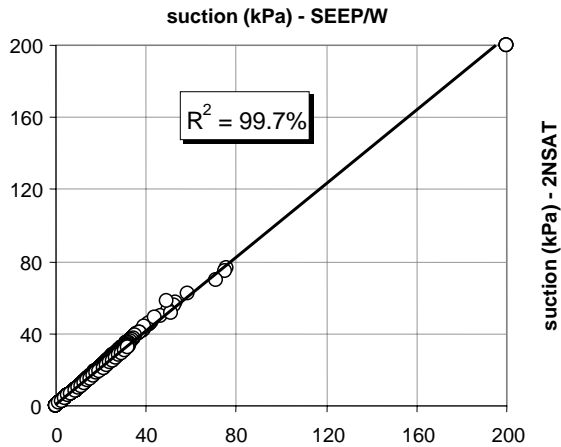
Fig. 7. A Comparison of the suctions obtained after solving the problem defined in table 2 with SEEP/W (Geo-Slope, 2002) and 2NSAT. A 32-day period was simulated.

Table 4. Water content of profiles 15, 18 and 21 (near façade) at different depths. Readings began to be taken on October 14, 2004, 3 days after completing profile installation.

depths (cm)	Profiles		
	15	18	21
10	0.342	0.343	0.345
20	0.342	0.341	0.343
30	0.341	0.341	--
40	0.340	0.340	--
50	0.336	0.339	0.339

The program has been applied to real cases. It was used to analyze the stabilization of 25 buildings in Rondilla Street in Alcazar de San Juan (central Spain). In the summer of 1997 construction work was carried out in this street, which entailed the opening of a wide trench (1.3 m width × 2.5 m depth) in the middle of the street to replace a sewage pipeline, and the excavation of two small service trenches (0.6 m width × 0.7 m depth) to lay the water mains and gas lines. Sixty-seven chinaberry trees (Melia 9ñAzedarach) were also planted. After the summer of 2003, which was especially hot and dry, the residents began to notice the aperture of cracks in their homes. According to the testimonies, these apertures advanced more rapidly in summer. This would make it unlikely that the damage would be linked to a shear mechanism, which is usually activated in winter with increased soil moisture. Only the shrinkage induced by the trees coincided with this seasonal characteristic.

As shown in Table, the model highlights the fact that the trees had very little impact on the moisture near the façades of the houses. Therefore, the settlements (vertical movements) of the footings were minor (see *v* in Fig. 5). In contrast, the shrinkage from summer transpiration gave rise to lateral movements (see Fig. 5), causing damage. Further analyses on the stability of the system showed that these deflections may not be the only cause of the damage. It is quite likely that the loss of confinement owing to the excavation of the service trench near the footings also played an important role. In any case, the evaluation of *u* and *v* (Fig. 5), as well as the characterization of moisture distribution (Fig. 6), served to orient the remedial works carried out. This entailed the selective transplantation of the chinaberries and the construction of a line of micropiles in the 25 buildings showing the greatest damage.

4.- Conclusions

A new tool for the characterization of soil-moisture changes caused by trees growing close foundations has been presented here. Although we used an idealization of the problem, the model put forth makes it possible to outline the functioning of the building-tree system schematically in a large number of cases.

This program was useful in supporting the identification of the damage mechanism in a real case of stabilization, playing a key role in the design of the remedial works. The case presented here is an example of the program's ability to provide support in engineering practice.

References

Alonso, E.E. y Lloret, A. 1995. Settlement of a 12 storey building due to desiccation induced by trees: a case study. En: Alonso, E.E. y Delage, P. (eds.) Proceedings of the first International Conference on Unsaturated Soils, Paris. 1995, 2, 935-943.

Allen, R.G., Pereira, L.S., Raes, D. y Smith, M. 1998. Crop evapotranspiration (guidelines for computing crop water requirements). FAO irrigation and drainage paper, 56, 290 p., Roma.

British Standard Institution (BSI). 1991. BS 5837: Guide for trees in relation to construction, British Standard Institution, 40 p., London.

Brooks, R.H. y. Corey A.T. 1964. Hydraulic Properties of Porous Media. Hydrology Paper, Colorado State Univ., Fort Collins.

Building Research Establishment (BRE). 1996. Damage to buildings caused by trees. BRE Good Repair Guide 2. BREPress. 8 p., Watford.

Building Research Establishment (BRE). 1999. Low-rise building foundations: the influence of trees in clay soils. BRE Digest 298. BREPress. 8 p., Watford.

Burdine, N.T. 1953. Relative permeability calculations from pore-size distribution data. Petr. Trans., Am. Inst. Mining Metall. Engng., 198, 71-77.

Canada Mortgage and Housing Corporation (CHMC). 2005. Understanding and dealing with interactions between trees, sensitive clay soils and foundations. About you house fact sheets, 62226, Canada Mortgage and Housing Corporation, 8 p., Ottawa

Carsel, R.F. y Parrish, R.S. 1988. Developing joint probability distributions of soil water retention characteristics. Water Resour. Res., 24, 755-769.

Feddes, R.A., Kowaklik, P.J. y Zaradny, H. 1978. Simulation of field water use and crop yield. John Wiley and Sons, 188 p.

Geo-Slope. 2002. Seep/W for finite element seepage analysis. User's guide (Version 5). Geo-Slope International, Canada, 549 p.

Indraratna, B., Fatahi, B. y Khabbaz, H. 2006. Numerical analysis of matric suction effects of tree roots. Proc. Inst. Civ. Eng., Geotech. eng., 159(2), 77-90.

Lloret, A. and Alonso, EE. 1985. State surfaces for partially saturated soils. Proc. 11th. Int. Conf. Soil Mech. and Fnd. Engng. San Francisco, 2, 557-562.

Mathur, S. 1999. Settlement of soil due to water uptake by plant roots. Int. J. Numer. Anal. Methods Geomech., 23(12), 1349-1357.

McKeen, R.G. 1992. A model for predicting expansive soil behaviour. The Proceedings of the Seventh International Conference on Expansive Soils, Dallas, 1992. Texas Tech University Press, Lubbock, USA, 1-6.

Meyer, P.D., Gee, G.W. y Nicholson, T.J. 1999. Information on hydrological conceptual models, parameters, uncertainty analysis, and data source for dose assessment and decommissioning sites. NUREG/CR-6656. U.S. Nuclear Regulatory Commission, Washington, DC, USA.

National House Building Council (NHBC). 1997.4.2. Building near trees: National House Building Council Standards. Amersham, NHBC.

Navarro, V., y Alonso, E. E. 2000. Modeling swelling soils for disposal barriers, Computers and Geotechnics, 27(1), 19-43.

Odenwald, N.G. y Welch W.C. 2004.Trees for Louisiana landscapes. A handbook. Available at the site www.lsuagcenter.com.

Seed H.B., Woodward R.J. Jr. y Lundgren, R. 1962. Prediction of swelling potential for compacted clays. J. Soil Mech. Found. Div., 88, SM3, 53-87.

Tratch, D.J., Wilson, G.W. y Fredlund, D.G. 1995. An introduction to analytical modelling of plant transpiration for geotechnical engineers. In Proceedings of the 48th Annual Canadian Geotechnical Conference, Vancouver, 1995. B.C., 2, 771-780.

Van Genuchten, M.T. 1980. A closed-form equation for predicting the hydraulic conductivity of unsaturated soils, Soil Sci. Soc. Am. J., 44, 892-898.

Zurich Municipal. 1996. Foundations-Proximity of Trees in Clay Soils. Zurich Municipal Builders' Guidance Note 3A. Zurich Municipal.